Optimization of 60 GHz three-port Grid Array Antenna

Zhao Wei[1], Sun Mei[2], Guo Yongxin[1]

[1]National University of Singapore, Singapore, 119077, Singapore

[2]Institute of Microelectronics (IME), ASTAR, Singapore, 138634, Singapore

***Abstract*— This paper proposes optimization methods for a 60GHz three-port Grid Array Antenna (GAA), aiming to optimize the return loss and Gain of the antenna. The working frequency range of the antenna is 57GHz~64GHz. After optimization, the GAA produces frequency scanning beams with 1~2dB Gain improvement when feeding at edge ports and boresight resonant beams with 2dB Gain improvement when feeding at the center port with Return Loss >11dB. The feature of frequency scanning and boresight resonant beams produced by this three-port GAA will find usage in 2D and 3D multi-mood Radar imaging applications.**

***Index Terms*— Grid Array Antenna (GAA), optimization**

I. Introduction

The GAA was first proposed by Kraus in 1964, and some studies have been studied since then by Nakano and his group [1] and Zhang's group [2-4]. Sun proposed a three-port GAA in 2020 [5]. When feeding at the edge this GAA works at traveling wave modes thus producing frequency scanning beams, which enables fast scanning 2D radar imaging applications; When feeding at the center this GAA works at resonant mode thus producing boresight beams, which enables 3D radar imaging applications.

In this paper, a three-port 60GHz GAA will be designed and optimized to cover 57-64GHz. Section II shows the GAA structure and optimization steps; Section III presents the optimization performance; Section IV summarizes conclusions.

II. GAA Structure and optimization steps

Fig.1 shows the cross-section, bottom view of the 60GHz three-port GAA, and top view of GAA before optimization and after optimization. Rogers 3003 is used for PCB substrate. The microstrip GAA consists of a rectangular grid of microstrip lines on a dielectric substrate, supported by a metallic ground plane. It is fed at three nodes by coaxial vias through apertures in the ground plane. For the radiator GAA meshes as shown in Fig. 1(b) l is the length of the long side, W is the length of the short side, w_l is the width of the long side, w_w is the width of the short side. Before optimization, l=3.14mm, W=1.8mm, w_w=w_l=0.2mm. It is noted in the optimization only GAA radiator is changed. The optimization steps are listed as below:

A. Step 1 – change the width of short side w_w

The width w_w is a key parameter used to control the isolation between two ports. A larger w_w results in higher isolation between Port 1 and 2 as well as Port 2 and 3 and a higher antenna gain [3]. In order to improve the Gain, it is important to change w_w. After comparison, choosing w_w=0.5mm as a compromise.

B. Step 2 – change the width of long side w_l

The width w_l controls transmission line loss and radiation from cross-polarized components [4]. The impedance matching is adjusted by changing the length of w_l. After choosing w_l=0.26mm, $|S_{11}|$, $|S_{22}|$, and $|S_{33}|$ have been optimized to a certain extent with Gain performance kept.

C. Step 3 – add matching stubs

Stubs are added to better match the input impedance to 50Ω as in Fig.1(c) as varied with locations. To maintain structural symmetry, matching stubs are symmetrical in the y-direction [6]. After adding matching stubs, $|S_{11}|$, $|S_{22}|$ and $|S_{33}|$ have been significantly improved while Gain performance kept.

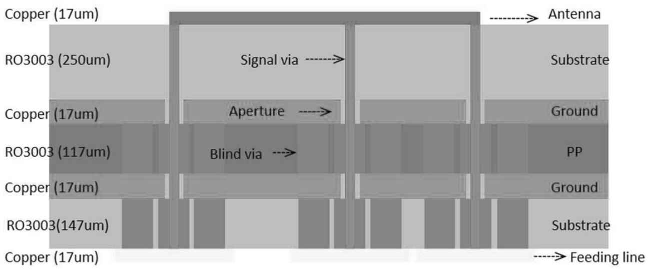

(a)

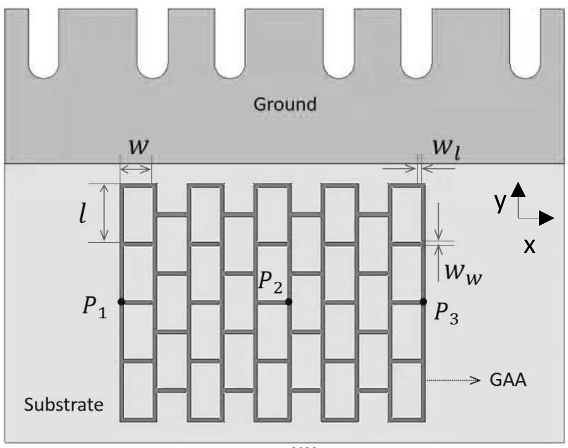

(b)

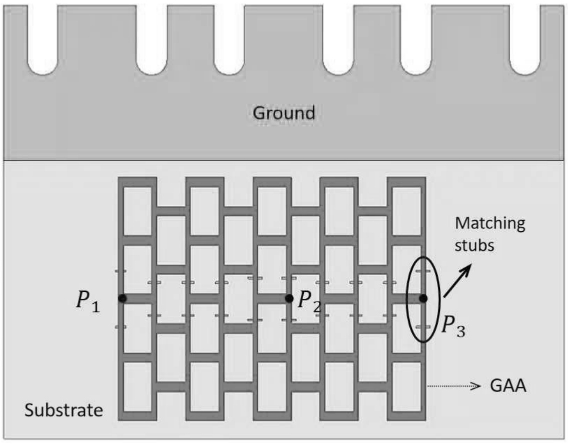

(c)

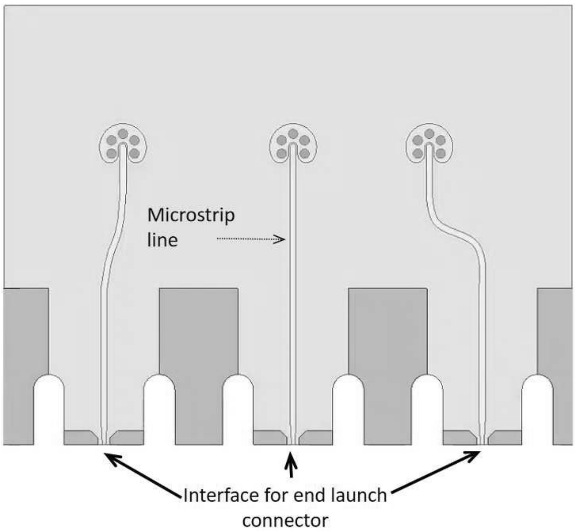

(d)

Fig. 1. Structure of 60GHz three-port GAA: (a) the cross-section, (b) the top view before optimization, (c) the top view after optimization, and (d) the bottom view.

I. GAA OPTIMIZATION PERFORMANCE

Fig.2 and Fig.3 show the comparison of impedance matching ($|S_{11}|$, $|S_{22}|$ and $|S_{33}|$) and realized Gain of the 60GHz three-port GAA before optimization and after Step 1, Step 2, and Step 3 optimization separately. $|S_{11}|$ is different from $|S_{33}|$ due to the unsymmetrical location of center port 2. It is shown that Gain increases with Step 1 w_w optimization however the return loss is getting worse; While with Step 2 of the change of w_l, the matchings have some improvements while also keeping Gain performance; After Step 3 of further adding matching stubs, $|S_{11}|$, $|S_{22}|$ and $|S_{33}|$ have been obviously improved while keeping Gain performance. After all three steps of optimization, the Gain at port 1 and port 3 is increased by 1~2dB, and the Gain at the center port (port 2) is increased by about 2dB over 57-64GHz with Return Loss >11dB for all ports.

Fig.4 shows the patterns of three-port GAA after optimization at XZ plane. When feeding at the edge at P1 and P3 this GAA works at traveling wave modes producing continuous frequency scanning beams over 57-64GHz, which enables fast scanning 2D radar imaging applications; When feeding at the center at Port 2 this GAA works at resonant mode producing boresight beams over 57-64GHz, which enables 3D radar imaging applications.

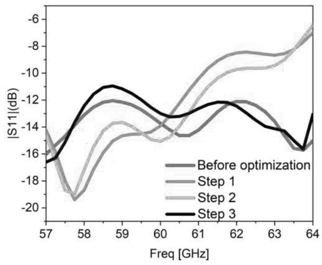

(a)

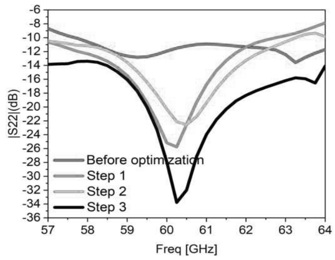

(b)

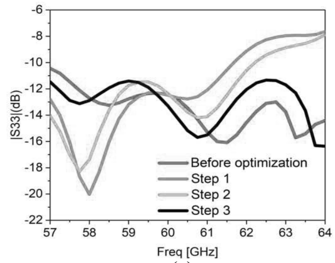

(c)

Fig. 2. S parameters performance: (a) $|S_{11}|$, (b) $|S_{22}|$ and (c) $|S_{33}|$.

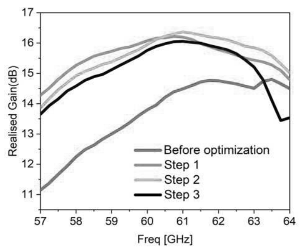

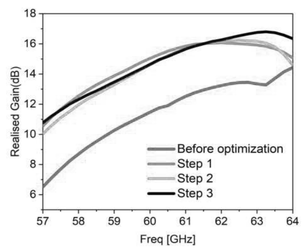

(a) (b)

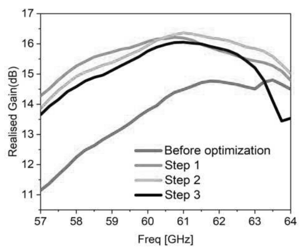

(c)

Fig. 3. Realized Gain performance: (a) P1 (b) P2 (c) P3.

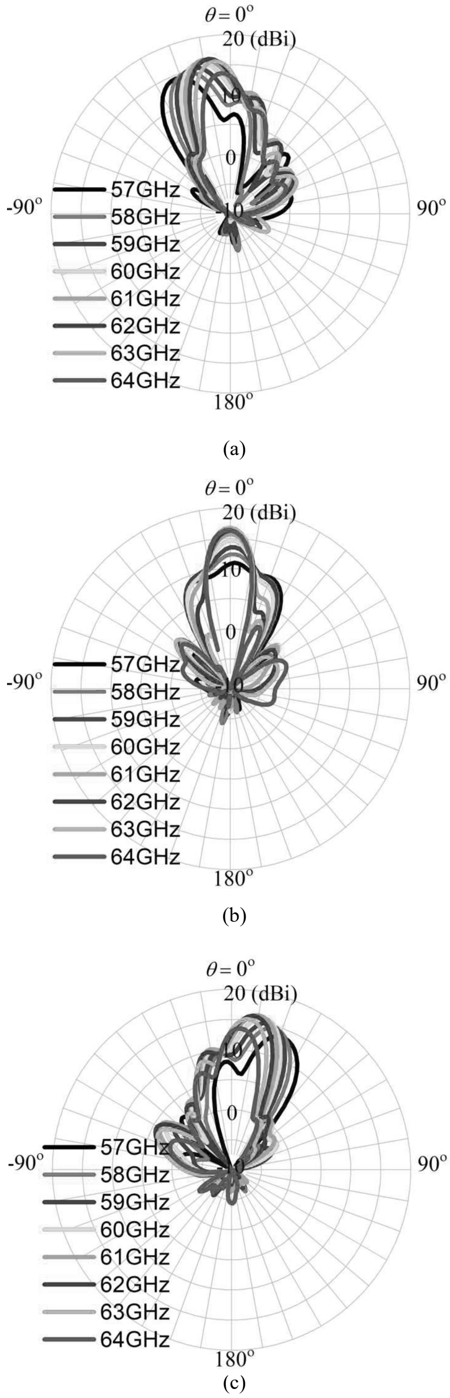

Fig. 4. Patterns at XZ plane after optimization: (a) P1 (b) P2 (c) P3.

I. CONCLUSION

The 60GHz three-port GAA in low-cost PCB technology has been designed and optimized. The optimization of the GAA radiator meshes includes changing the short side width to increase the Gain, changing the long side width to further slightly improve the matching, and adding matching stubs to finally improve impedance matching greatly while keeping Gain performance. The optimized GAA has demonstrated the frequency scanning beams with 1~2dB Gain improvement when feeding at edge ports as well as boresight resonant beams with 2dB Gain improvement when feeding at the center port with Return Loss >11dB. These features enable three-port GAA to find usage in 2D and 3D multi-mood Radar imaging applications.

ACKNOWLEDGMENT

This research is supported by A*STAR C211718010: Urban and Green Technology Horizontal Technology Coordinating Office (UGT HTCO) Seed Fund project. The authors greatly appreciate the members' and collaborators' participation in discussions and encouragement throughout the project which makes this research possible.

REFERENCES

[1] H. Nakano, T. Kawano, Y. Kozono, J. Yamauchi, "A fast MoM calculation technique using sinusoidal basis and testing functions for a wire on a dielectric substrate and its application to meander loop and grid array antennas," IEEE Trans. Antennas Propagat., vol. 53, no. 10, pp. 3300-3307, October 2005.

[2] M. Sun and Y. P. Zhang, "A 60-GHz LTCC microstrip grid array antenna," 2010 Asia-Pacific Microwave Conference, Yokohama, Japan, 2010, pp. 1673-1676.

[3] Z. Chen, Y. P. Zhang, A. Bisognin, D. Titz, F. Ferrero and C. Lux-ey, "A 94-GHz Dual-Polarized Microstrip Mesh Array Antenna in LTCC Technology," in IEEE Antennas and Wireless Propagation Letters, vol. 15, pp. 634-637, 2016.

[4] Z. Chen and Z. Y. Ping, "24-GHz microstrip grid array antenna for automotive radars application," 2015 IEEE 5th Asia-Pacific Conference on Synthetic Aperture Radar (APSAR), 2015, pp. 125-127.

[5] M. Sun, et al. "Antenna and method of forming the same," US20200358205A1.

[6] R. Gopika and C. Saha, "Millimeter Wave Grid Array Antenna for Wireless Power Transmitter," 2019 IEEE Recent Advances in Geoscience and Remote Sensing : Technologies, Standards and Applications (TENGARSS), 2019, pp. 54-56.